nature neuroscience

Dopamine modulates an mGluR5-mediated depolarization underlying prefrontal persistent activity

Kyriaki Sidiropoulou[1,6], Fang-Min Lu[2], Melissa A Fowler[2], Rui Xiao[3], Christopher Phillips[2], Emin D Ozkan[2], Michael X Zhu[3], Francis J White[4,5] & Donald C Cooper[2]

The intrinsic properties of neurons that enable them to maintain depolarized, persistently activated states in the absence of sustained input are poorly understood. In short-term memory tasks, individual prefrontal cortical (PFC) neurons can maintain persistent action potential output during delay periods between informative cues and behavioral responses. Dopamine and drugs of abuse alter PFC function and working memory, possibly by modulating intrinsic neuronal properties. Here we used patch-clamp recording of layer 5 PFC pyramidal neurons to identify a postsynaptic depolarization that was evoked by action potential bursts and mediated by metabotropic glutamate receptor 5 (mGluR5). This depolarization occurred in the absence of recurrent synaptic activity and was reduced by a dopamine D1 receptor (D1R) protein kinase A pathway. After behavioral sensitization to cocaine, the depolarization was substantially diminished and D1R modulation was lost. We propose that burst-evoked intrinsic depolarization is a form of short-term cellular memory that is modulated by dopamine and cocaine experience.

The PFC is a highly evolved brain region closely linked to attention and working memory in primates and rodents[1,2]. Drugs of abuse, such as cocaine, are known to disrupt attentional and working memory processes, but the mechanism is unknown[3,4]. In fact, little is known about the basic neuronal and network properties that sustain attention and working memory in general. In working memory tasks, pyramidal neurons in the PFC are capable of maintaining action potential output during delay periods between an informative cue presentation and the appropriate behavioral response[5]. The induction of persistent action potential activity may hold information necessary to guide goal-directed behavior in memory until it is no longer necessary (for example, after a response or reward). Several computational approaches have been put forth to explain delay period activity, ranging from highly abstract models to biophysically detailed conductance-based models. Most modeling studies of persistent activity have focused on recurrent network models[6]. These models require precise tuning and weighting of synaptic inputs to maintain stable persistent activity and are limited by minimal biophysical validity and pronounced susceptibility to interference[6,7]. The robustness and resistance to mistuning of these models can be substantially improved mathematically by prolonging the synaptic decay time constants or incorporating cellular bistability that allows neurons to fluctuate between hyperpolarized resting and depolarized activated states[6,7]. Strong bursts of synaptic stimulation and concomitant activation of NMDA channels, voltage-gated Ca^{2+} channels and Ca^{2+}-activated nonselective cation channels could provide the biological mechanism necessary to maintain activated states under conditions of diminishing excitatory drive during the delay period[7–9].

We used an experimental approach to identify an intrinsic mechanism capable of converting subthreshold inputs into persistent suprathreshold output for several seconds in deep-layer PFC pyramidal neurons. To date, research on the role of glutamate in working memory has mainly focused on the fast, excitatory ionotropic AMPA and NMDA glutamate receptors; recently, however, the group 1 G protein–coupled mGluRs and their slow excitatory transmission have gained attention owing to their role in controlling prefrontal cortical activity, working memory processes, psychostimulant reward and hippocampal and cerebellar synaptic plasticity[10–15].

From a circuit perspective, several inputs converge onto layer 5 pyramidal neurons of the PFC, including local PFC inputs; hippocampal, subicular and mediodorsal thalamic glutamatergic inputs and dopamine (DA) input from the ventral tegmental area[16,17]. Extracellular DA levels increase in the PFC during working memory tasks in primates and rats[18,19]. Furthermore, an optimal level of activation of the D1 class dopamine receptors (D1R) is important for proper performance on PFC-dependent working memory tasks[20]. D1Rs modulate PFC neuronal activity both *in vivo*[20,21] and *in vitro*[22–26], where they have been reported to exert inhibitory and excitatory effects. For example, D1Rs interact with NMDA receptors to enhance cellular excitability[22] and mGluRs to induce long-term depression[13]. mGluR5

[1]Department of Neuroscience, Rosalind Franklin University of Health and Science/Chicago Medical School, 3333 Green Bay Road, North Chicago, Illinois 60064, USA. [2]Department of Psychiatry, University of Texas Southwestern Medical Center, 5323 Harry Hines Boulevard, Dallas, Texas 75390-9070, USA. [3]Department of Neuroscience and Center for Molecular Neurobiology, Ohio State University, 206 Rightmire Hall, 1060 Carmack Road, Columbus, Ohio 43210, USA. [4]Department of Cellular and Molecular Pharmacology, Rosalind Franklin University of Health and Science/Chicago Medical School, 3333 Green Bay Road, North Chicago, Illinois 60064, USA. [5]Deceased. [6]Present address: Computational Biology Lab, Institute of Molecular Biology and Biotechnology, Foundation for Research and Technology–Hellas, Vassilika Vouton, GR71110, Greece. Correspondence should be addressed to D.C.C. (don.cooper@live.com).

Received 3 November 2008; accepted 26 November 2008; published online 25 January 2009; doi:10.1038/nn.2245

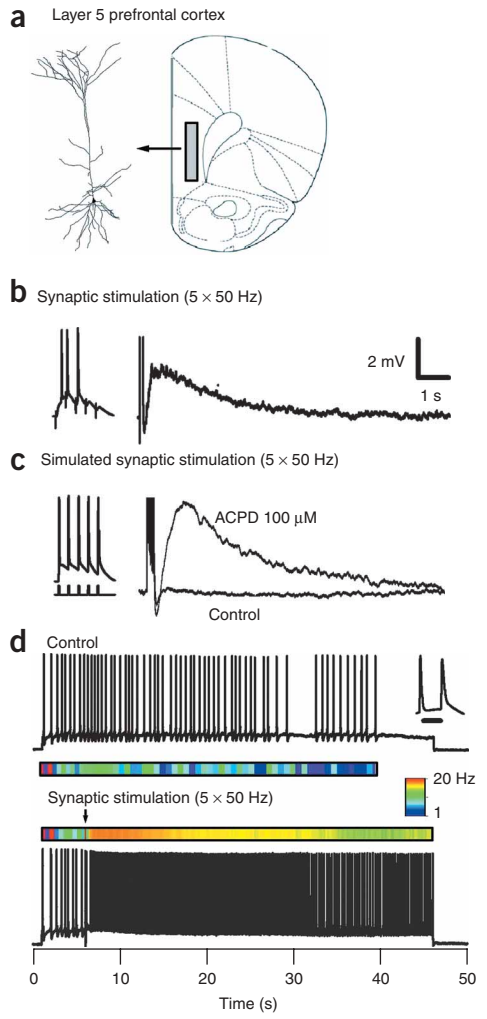

Figure 1 Patch-clamp recording from layer 5 pyramidal PFC neurons showing mGluR-activated dADP and persistent activity. (**a**) Left, Neurolucida reconstruction of a representative PFC layer 5 pyramidal neuron filled with 0.1% biocytin. Right, deep layer 5 and 6 regions in prelimbic and infralimbic regions (shaded area) of PFC where recordings were made. (**b**) Voltage response of layer 5 pyramidal PFC neuron after synaptic stimulation with stimulating electrode positioned along apical dendrite in cortical layer 3. Left, a single burst of synaptic stimulation (5 × 50 Hz) induced dADP in presence of $GABA_A$ and $GABA_B$ (SR 95531, 2 μM) and AMPA and NMDA (kynurenic acid, 2.5 mM) blockade. (**c**) In presence of mGluR agonist ACPD (100 μM), a single burst of five brief (2 ms) suprathreshold current step pulses (left) elicited a dADP with kinetics similar to synaptically activated dADP in the presence of GABA and ionotropic glutamate blockers (see Methods). Scale bar in **b** also applies to **c**. (**d**) Action potential activity from bursting (inset, 10-ms scale bar) layer 5 pyramidal neuron in response to a 45-s suprathreshold current step. Color map below trace shows instantaneous firing rate that averaged ~2.2 Hz. A single burst of spike-triggering synaptic stimulation induced pronounced increase in instantaneous firing rate that was sustained for the duration of current step injection. Color map shows instantaneous firing rate change from 1 to 20 Hz.

has recently been implicated in PFC-dependent executive functions because inhibition of mGluR5 impairs working memory[10]. It is clear that a proper balance of glutamate and DA tone is important for working memory and executive cognitive control, all of which can be disrupted by exposure to psychostimulant drugs of abuse, like amphetamine and cocaine[3,4,10,18–21,27].

The goals of this study were to identify a Ca^{2+}-dependent postsynaptic mGluR-mediated delayed afterdepolarization (dADP) mechanism capable of providing sustained activity in deep-layer PFC pyramidal neurons, test whether this dADP could be modulated by postsynaptic D1R- or D2R-family signaling cascades and determine whether a behavioral sensitizing regimen of cocaine would lead to long-lasting disruption of this mechanism.

RESULTS

mGluR activation induces burst-triggered dADP

A single burst of gamma-frequency (~20–50 Hz) synaptic stimulation induced a mGluR-mediated, calcium-dependent dADP capable of converting subthreshold input and low-frequency activity to prolonged action potential output lasting tens of seconds in layer 5 pyramidal neurons of the rat PFC (**Figs. 1** and **2a** and **Supplementary Figs. 1** and **2** online). Because most (>90%) fast excitatory transmission was blocked, we hypothesized that the delayed cellular response was due to activation of mGluRs.

To test the role of postsynaptic mGluRs more directly, we triggered action potentials with brief current injections through the patch pipette that induced a dADP in the presence of mGluR agonists (1*S*,3*R*)-1-amino-cyclopentane-1,3-dicarboxylate (ACPD; 100 μM) or *S*-3,5-dihydroxyphenylglycine (DHPG; 50–100 μM), applied either locally with a puffer pipette (150 μm from the base of the apical dendrite) or in the bath (**Fig. 1c**). At a broad range of frequencies (2–100 Hz), bursts of two or more action potentials were more effective than single spikes at producing the dADP (**Supplementary Fig. 1**). The dADP amplitude and integral was independent of the frequency but was dependent on the number of spikes, which saturated the dADP after four spikes ($n = 6$; **Supplementary Fig. 1**). Using a physiologically relevant simulated synaptic stimulus that triggered five action potentials delivered at 50 Hz, the ACPD-induced dADP had an average amplitude of 3.7 ± 0.6 mV, peaked at 1.2 s and decayed with a time constant of 2.5 ± 0.3 s ($n = 19$). Synaptic activation of 5 and 30 stimuli (50 Hz) delivered between 100 and 200 μm from the soma along the apical dendrite produced a similar prominent dADP in the presence of fast synaptic blockers in 7 (64%) of 11 pyramidal neurons. Thirty stimuli produced a slightly larger response than did five pulses for dADP peak (4.6 ± 0.8 mV ($n = 5$) for 5 stimuli versus 7.9 ± 0.9 mV ($n = 7$) for 30 stimuli; $P < 0.03$) and integral and instantaneous frequency (**Supplementary Fig. 2**).

In vitro simulation of *in vivo* conditions

To understand how the mGluR-induced dADP influences action potential dynamics under simulated *in vivo* conditions, we delivered time-varying current inputs in the presence of brief local or bath-applied mGluR agonist. To test the ability of the dADP to maintain spike output under simulated *in vivo* conditions in the presence of ongoing action potential activity, we programmed an ascending ramp stimulus that simulated the rising excitatory drive associated with attending to an informative stimulus, and a descending ramp to simulate the diminished excitation that occurs after stimulus withdrawal in a behavioral task. Time-varying stimuli, like depolarizing ramp current injections, have been used to characterize cortical pyramidal neurons *in vitro* to mimic the type of input likely to be present *in vivo* as correlates of preparatory and anticipatory processes in sensorimotor and cognitive behaviors[28]. Progressively depolarizing and hyperpolarizing inputs are common in cortical parietal and frontal regions and could participate in muscular recruitment, response preparation and decision-making processes[28].

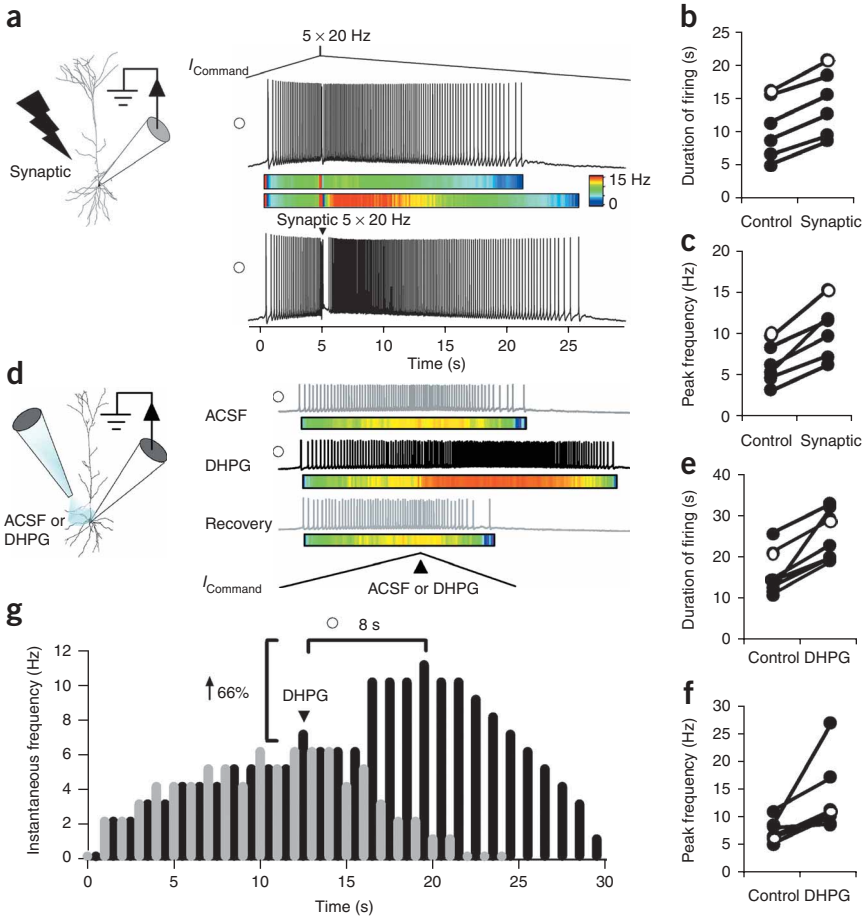

Figure 2 Patch-clamp recording from layer 5 pyramidal PFC neurons showing response to an ascending and descending input stimulus before and after mGluR activation. (**a**) Proximal apical dendritic synaptic stimulation and recording and Neurolucida reconstruction of a biocytin-filled layer 5 pyramidal neuron. Top right, representative trace showing the response to a 5-s ascending and 40-s descending ramp with a burst stimulus (5 × 20 Hz) current command. Under control conditions, instantaneous firing rate follows current command input. Bottom right, enhanced response to a synaptic burst stimulus (5 × 20 Hz) delivered at the peak of the ramp. Open circle represents cell shown in **b** and **c**. Color map shows instantaneous frequency (0–15 Hz) before and after synaptic stimulation at the peak of the ramp. (**b**,**c**) Increased duration of action potential firing ($n = 7$; $P < 0.001$) during the descending ramp and increased instantaneous firing rate ($n = 7$; $P < 0.001$) after a burst of five synaptic stimuli compared to five brief current injections delivered at the peak of the ramp. Open circle shows a representative neuron from **a**. (**d**) Double-barreled pipette located 50 μm from soma was filled with ACSF in one barrel and DHPG in the other (both 100 μM) and used to puff on the soma and proximal apical and basilar dendrites. Whole-cell patch-clamp pipette is also shown. Gray trace shows representative action potential response to an $I_{Command}$ ramp stimulus (40 s ascending and 40 s descending) and brief 1-s pressure application of ACSF at the peak of the ramp (black arrow). Black trace shows action potential response of the same cell with 1-s application of DHPG (100 μM; black arrow) at peak of $I_{Command}$. Recovery trace puffing ACSF was taken 30 s after DHPG. (**e**,**f**) Increased duration of action potential firing during descending ramp ($n = 7$; $P < 0.005$) and increased instantaneous firing rate ($n = 7$; $P < 0.02$) after 1-s puff of DHPG compared to control ACSF puff. (**g**) Ramp induced spiking in response to pressure application of control ACSF (gray) or DHPG (black) delivered at peak of ramp (black arrow). Instantaneous frequency histogram (1-s bins) for traces shown in raster plot is shown with time 0 set to onset of the first spike. Peak frequency after DHPG in this recording occurred 8 s after peak of ramp current stimulus. Open circle shows representative recording in **e** and **f**.

At the peak of the ascending ramp current command ($I_{Command}$), we pressure-applied artificial cerebrospinal fluid (ACSF) alone or ACSF with 100 μM DHPG using a patch pipette (3 MΩ) for 1 s, and we monitored spike output during the falling phase of the ramp stimulus (**Fig. 2**). We adjusted the ramp current injection before mGluR activation to produce peak sustained firing rates between 3 and 12 Hz to correspond to realistic *in vivo* cortical baseline firing rates[29]. Under these conditions, mGluRs were activated among a background of action potential activity, as seen *in vivo*. Compared to current injection alone, brief synaptic stimulation of 5–30 pulses delivered at 20–50 Hz produced a robust increase in the duration (40 ± 7%; $P < 0.005$) and instantaneous frequency (68 ± 12%; $P < 0.005$) of action potential firing (**Fig. 2a–c**). We obtained similar results using local postsynaptic DHPG puff application, which produced a robust increase in the instantaneous frequency (85 ± 25%; $n = 7$, $P < 0.01$), and duration (64 ± 18%; $n = 7$, $P < 0.005$; **Fig. 2d–g**) of action potential firing. All seven cells responded to the DHPG puff, and all baseline responses fully recovered within 30 s of DHPG application (**Fig. 2d**). Thus, brief postsynaptic activation of mGluRs can prolong and increase the frequency of spike output even in the presence of descending excitatory input (that is, the firing frequency reaches a delayed maximum firing rate that peaks several seconds after the peak of excitatory input).

Activation of group 1 mGluRs leads to increases in intracellular Ca^{2+} in neurons, an effect greatly enhanced by simultaneous action potential generation and/or cellular depolarization[9,11,15,30,31]. To determine a necessary role for intracellular Ca^{2+}, we used 1,2-bis-(*o*-amino-phenoxy)ethane-*N*,*N*,*N*′,*N*′-tetraacetic acid (BAPTA; 5–10 mM) in the recording pipette and monitored the dADP and action potential–triggered action potential activity in the presence of DHPG. BAPTA produced a substantial reduction in the dADP (**Fig. 3a,b**; $n = 5$, $P < 0.01$), as we previously reported[9]. The functional consequence of the dADP on action potential output was more obvious when we introduced subthreshold membrane potential fluctuations by replaying a previously recorded near-threshold current stimulus command input to mimic the background *in vivo* activity[32]. In the subthreshold domain, mGluR activation had no significant effect, as detected by a low-frequency noise current stimulus in the prespike period that produced a 24.7 mV span from –80 mV to –55.3 mV (**Fig. 3c**). In contrast, after a single action potential or doublet burst, mGluR activation converted the subthreshold noise input into prolonged spike output that was completely eliminated by intracellular Ca^{2+} chelation with BAPTA (**Fig. 3c,d**; $n = 7$, $P < 0.01$). This indicates the Ca^{2+}-dependent nature of the mGluR-induced dADP and its ability to convert brief bursts of activity into sustained output. The sustained activity was maintained even during brief periods (~100 ms) of hyperpolarization below the resting potential (**Fig. 3c**), demonstrating that the dADP action potential amplification mechanism is resistant to transient inhibitory interference.

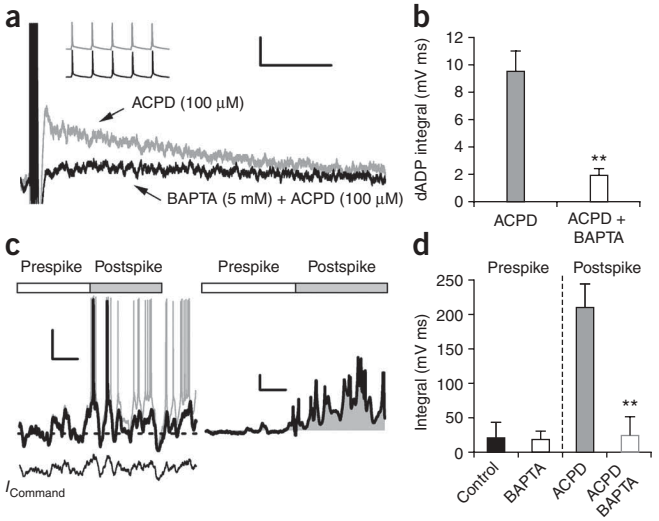

Figure 3 The dADP requires intracellular Ca^{2+} and can amplify and convert near-threshold inputs into sustained output only after an initial action potential. (**a**) Chelation of intracellular Ca^{2+} with BAPTA (5 mM) substantially reduced burst-triggered dADP in the presence of mGluR agonist ACPD (100 μM). Inset shows no differences in a dADP-inducing burst of five action potentials after ACPD after initial break-in to whole-cell mode or 15 min after intracellular perfusion with BAPTA. Scale bars show 1 mV and 2 s. (**b**) BAPTA significantly reduced area under curve (integral) of dADP triggered by burst of action potentials in the presence of bath-applied ACPD ($n = 5$; $^{**}P < 0.01$). (**c**) Left, subthreshold recording from pyramidal neuron was played back as $I_{Command}$ and scaled to produce an action potential (black trace). ACPD (100 μM) was applied by pressure injection from 10 s before the sweep until the end (gray trace). Washout of ACPD 30 s after DHPG application indicated rapid recovery to baseline response (data not shown). Scale bars show 20 mV and 1 s. Right, subtraction of ACPD trace (gray) from baseline (black) shows amplification of subthreshold activity during postspike period. Action potentials, which comprised a very small component of the postspike integral, accounted for <5% of total area and were subtracted from total integral calculation as shown. Scale bars show 5 mV and 1 s. (**d**) Baseline subtraction of prespike membrane potential interval (3 s) compared to postspike membrane potential interval (3 s) after puffed ACPD (100 μM; $n = 4$) or DHPG (100 μM; $n = 3$) application (BAPTA alone, $n = 6$; pooled, $n = 7$; $^{**}P < 0.01$). Error bars represent s.e.m.

Burst-triggered dADP depends on mGluR5 activation

To determine which mGluR is responsible for the dADP, we used pharmacological and gene-deletion approaches. Group 2 mGluRs were not involved in dADP induction, as bath application of a selective concentration of the group 2 antagonist LY341495 (20 nM) did not significantly change the ACPD-induced dADP amplitude ($n = 6$, $P = 0.27$). Group 1 mGluRs seemed to mediate the dADP, as a higher concentration of the group 1 and 2 mGluR antagonist LY341495 (20 μM) significantly decreased the dADP amplitude from 6.6 ± 0.1 mV to 3.0 ± 0.4 mV ($P < 0.002$). The group 1 mGluR agonist DHPG (50 μM) induced the burst-triggered dADP with an average amplitude of 3.4 ± 0.2 mV, peak at 1.5 ± 0.04 s and decay-time constant of 3.4 ± 0.3 s ($n = 15$).

To dissect which group 1 mGluR is responsible for the burst-triggered dADP, we applied the selective mGluR1 receptor antagonist LY367385 (10 μM), which did not significantly decrease the dADP ($n = 6$, $P = 0.6$). In contrast, blockade of mGluR5 with the selective mGluR5 antagonist 2-methyl-6-(phenylethynyl)-pyridine (MPEP; 10–30 μM) produced a significant 60% decrease in the DHPG-induced dADP amplitude ($n = 6$, $P < 0.01$; **Supplementary Fig. 2**). This suggested that mGluR5 is responsible for the dADP, but pharmacological blockade of mGluR5 did not completely abolish the DHPG-induced dADP. We therefore tested the DHPG-induced dADP in two groups of knockout mice lacking mGluR1 or mGluR5 (**Fig. 4**). Using voltage- and current-clamp recording, we isolated DHPG-induced current (I_{DHPG}) and dADP, respectively, in mGluR1-knockout mice and found no differences compared to wild-type littermate controls ($n = 9$–11, $P > 0.05$; **Fig. 4a,b**), indicating a lack of mGluR1 involvement. In contrast, both the I_{DHPG} and dADP were completely abolished in the mGluR5-knockout mice ($n = 9$–11, $P < 0.01$; **Fig. 4c–f**), indicating that both the I_{DHPG} and burst-elicited dADP are mediated by mGluR5.

D1–protein kinase A modulation of mGluR5-mediated dADP

In the presence of DA (10 μM), the DHPG-induced dADP amplitude was significantly decreased ($n = 8$, $P < 0.05$; **Fig. 5**). Other properties of the dADP, such as the time to peak or kinetics of decay, remained unchanged. To determine whether bath-applied DA can reduce the synaptically triggered dADP, we tested the effects of DA on cells responding to synaptically elicited dADP. As with bath-applied DHPG, the synaptically triggered dADP was reduced ~50% by DA (10 μM). Because DA can reduce presynaptic glutamate release, we monitored the fast excitatory postsynaptic potentials (EPSPs) and paired pulse ratio and found that at this low concentration (10 μM) of DA, there was a significant—albeit small—11% reduction in the fast EPSP (**Fig. 5b–d**) and a 20% reduction in the paired pulse ratio ($n = 5$, $P < 0.05$). A similar reduction in paired pulse ratio, mediated by D1R , was reported in a study recording PFC pyramidal neuron pairs under similar experimental conditions[33]. To compensate for the slightly reduced fast EPSP in the presence of DA, we increased the stimulation intensity to effectively normalize the EPSP response before delivering the dADP-triggering burst of synaptic stimulation (**Fig. 5b–d**). After adjusting the synaptic stimulation intensity in the presence of DA, we still observed a substantial reduction in the dADP. The finding that synaptically elicited dADP was reduced by ~50%, whereas the fast EPSP was reduced by only 11%, indicated that the dADP is a more sensitive target for DA modulation than the fast AMPA-mediated EPSP (**Fig. 5b–d**).

To determine which receptor is responsible for DA actions on the dADP, selective agonists of the two different receptor classes were used. Activation of D2R using the D2-selective agonist quinpirole (10 μM) exerted no effect on the dADP integral in the presence of DHPG ($n = 8$, $P > 0.4$; **Fig. 5**). In contrast, application of the full D1R agonist SKF81297 (1-10 μM) mimicked the effect of DA application, producing a significant decrease in the dADP integral ($n = 28$, $P < 0.002$; **Fig. 5**). The effect of SKF81297 was prevented by prior application of the D1R antagonist SCH23390 (5 μM), indicating that the effect of SKF81297 was receptor mediated (**Supplementary Fig. 3** online). No differences were found between 1 and 10 μM SKF81297; however, an inverted U-shaped dose-response curve was observed across a full dose response from 0.5 to 50 μM SKF81297 (**Supplementary Fig. 3**). This is notable because a D1R-mediated inverted U-shaped dose-response curve has been noted in PFC working memory tasks, with optimal levels of D1R stimulation capable of facilitating performance on these tasks[20].

Stimulation by D1R reduces current through voltage-gated Na^+ channels in PFC pyramidal neurons[25]. Furthermore, behavioral sensitization to cocaine reduces whole-cell Na^+ current in the accumbens[33]. Despite these findings, D1R modulation of the mGluR-mediated dADP was independent of Na^+ channel function (**Supplementary Fig. 3**). To determine whether D1R activation reduces the dADP by attenuating dendritic backpropagating action potentials initiated by the burst, we applied a low concentration of tetrodotoxin (15 nM) that inhibits a

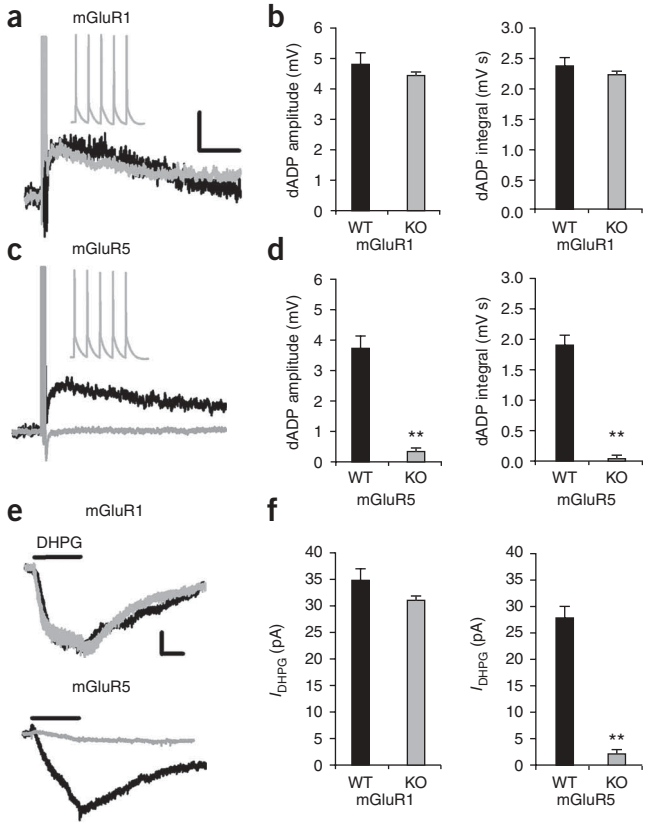

Figure 4 Burst-induced dADP is mediated by mGluR5. (**a**) Superimposed representative traces showing dADP induced by burst (five spikes, 50 Hz) after application of DHPG (100 μM) in wild-type mice (black trace) and mGluR1-knockout (KO) mice (gray trace). Scale bars show 2 mV and 2 s. Inset shows five action potentials during a burst in mGluR1-knockout mice. (**b**) Mice lacking mGluR1 showed normal DHPG-mediated, burst-induced dADP amplitude (left) and integral (right) compared to wild-type littermate controls ($n = 11$, $P = 0.8$). (**c**) Overlay of representative traces of burst-triggered dADP with DHPG in wild-type mice (black trace) and without DHPG in mGluR5-knockout mice (gray trace). (**d**) Compared to wild-type littermate controls, mGluR5-knockout mice (black trace) did not show DHPG-mediated, burst-induced dADP (left, amplitude, $n = 9$, $^{**}P < 0.01$; right, integral, $n = 9$, $^{**}P < 0.01$). (**e**) Top, average current induced by 30-s local puff application of DHPG (100 μM) 50 μm from soma of PFC pyramidal neurons held at –70 mV in wild-type mice (black trace) and mGluR1-knockout mice (gray trace). Bottom, absence of DHPG induced a slow inward cation current (I_{DHPG}) in mGluR5-knockout mice compared to wild-type controls. Scale bars show 10 pA and 10 s. (**f**) Average I_{DHPG} from wild-type and mGluR1-knockout mice (left; $n = 9$–11, $^{**}P > 0.05$) and wild-type and mGluR5-knockout mice (right; $n = 9$–11, $^{**}P < 0.01$) in response to 30-s pressure application of DHPG. Error bars represent s.e.m.

substantial (~60%) fraction of Na^+ channels while minimally reducing somatic action potential height (~5%)[34]. As we reported previously using high concentrations of tetrodotoxin (500 nM)[9], 15 nM tetrodotoxin was unable to alter the DHPG-induced, burst-triggered dADP or the inhibitory effects of D1R on dADP ($n = 28$ for SKF81297 alone, $n = 6$ for tetrodotoxin and SKF81297, $P > 0.05$; **Supplementary Fig. 3**). This result suggest that the burst and mGluR5-mediated dADP source is located near the soma and proximal dendrites.

D1Rs couple to G_s proteins, which increase cAMP levels and activate protein kinase A (PKA)[26]. To determine whether a PKA mechanism is involved in mediating the effects of SKF81297, we used forskolin (10 μM), an activator of adenylyl cyclase and PKA. Bath application of forskolin induced a significant decrease in the DHPG-induced dADP integral (**Fig. 5**). Application of the PKA blocker, N-[2-((p-Bromocinnamyl)amino)ethyl]-5-isoquinolinesulfonamide (H89; 10 μM) prevented the reduction in the DHPG-induced dADP integral caused by SKF81297 (**Fig. 5**). To confirm that the effects of SKF81297 and H89 were mediated through the PKA pathway, we assessed PKA phosphorylation of Thr34 on the dopamine- and cAMP-regulated phosphoprotein (DARPP-32), which showed a significant increase in phosphorylation after slices were incubated for 10 min in SKF81297 (10 μM; **Fig. 5**). As we observed with patch clamp recording, preincubation of PFC slices in H89 (10 μM) eliminated the effects of SKF81297 on the PKA site of DARPP-32 (**Fig. 5**). It is possible that D1Rs can couple to a PKC mechanism[26]. However, three findings argue against such a mechanism. First, the PKC inhibitor 2-[1-(3-Dimethylaminopropyl)-1H-indol-3-yl]-3-(1H-indol-3-yl)-maleimide (BMI) (1–50 μM) did not reduce the SKF81297-induced inhibition ($n = 5$, $P > 0.05$). Second, the PKA inhibitor H89 completely blocked the effects of SKF81297 (**Fig. 5**). Finally, forskolin completely occluded the effects of SKF81297, whereas it did not occlude the PKC-induced reduction of the dADP ($n = 5$, $P > 0.05$; data not shown).

To examine the synaptically triggered dADP and show that the effects of forskolin were postsynaptic, we used forskolin (10 μM) inside the patch pipette and monitored the synaptically triggered dADP (**Fig. 5a** and **Supplementary Fig. 4** online). Internal forskolin produced a significant reduction in the dADP that was similar to that induced by bath-applied DA, SKF81297 and forskolin (**Fig. 5a**). The intracellular Ca^{2+} response of heterologously expressed mGluR5 to DHPG was inhibited ~40% by forskolin (10 μM; **Supplementary Fig. 4**). These experiments rule out a presynaptic PKA contribution and show that postsynaptic PKA activation is sufficient to inhibit mGluR5-induced intracellular calcium release.

Plasticity of the dADP after repeated cocaine exposure

Repeated noncontingent injections of cocaine (5×15 mg kg^{-1} intraperitoneal) have been shown to induce plasticity of intrinsic excitability in the PFC[24]. We found that repeated cocaine treatment (5 d) and short-term (2 d) and long-term (14 d) withdrawal induce behavioral sensitization to a cocaine challenge injection in cocaine-treated compared to saline-treated rats ($n = 6$ per group, $P < 0.05$; **Fig. 6a**). Short-term withdrawal from cocaine produced a substantial reduction in the ability of elicit the dADP, despite a significant increase in measured input resistance observed in the cocaine group ($n = 21$–22 per group, $P < 0.03$; **Figs. 6** and **7** and **Supplementary Table 1** online). The diminished cocaine-induced dADP was accompanied by a complete loss of the inhibitory effects of D1R stimulation ($n = 7$–8 per group, $P < 0.001$; **Fig. 6c**). After long-term withdrawal, the dADP recovered in the cocaine-treated group ($n = 13$–15 per group, $P > 0.05$; **Fig. 6d**), but D1R modulation was still absent ($n = 11$ per group, $P < 0.03$; **Fig. 6d**). These results are consistent with our previous work in deep-layer PFC neurons showing that repeated cocaine and short-term withdrawal leads to increased basal PKA activity and intrinsic changes in ion channel function[24]. D1R pathway modulation of the dADP was absent at both withdrawal times, yet the cocaine-induced reduction in the dADP recovered fully after longer withdrawal, suggesting independent or compensatory mechanisms in the PKA pathway during withdrawal from cocaine.

Among the functional implications of the burst-induced dADP (**Fig. 7**) is its ability to convert near-threshold simulated synaptic inputs (**Fig. 7a**) to suprathreshold output for up to 4 s after the burst. We previously used simulated synaptic current injections designed to match the kinetics of the synaptically elicited fast EPSPs to probe

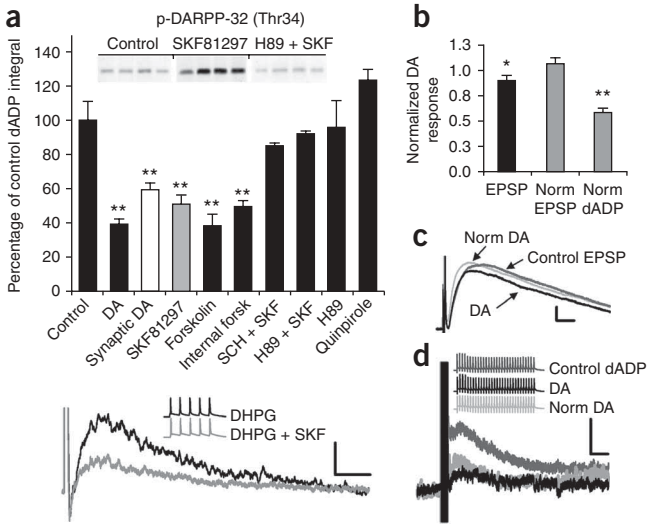

Figure 5 Dopamine reduces mGluR5- and burst-induced dADP through D1R-PKA pathway. (**a**) Top, DA ($n = 8$, $^{**}P < 0.01$) reduced the DHPG-mediated, burst-triggered dADP ('Control'; $n = 30$) and synaptically triggered dADP ('Synaptic DA'; $n = 6$, $^{**}P < 0.01$). D2 agonist quinpirole (10 μM) did not modulate dADP ($n = 8$), whereas D1R agonist SKF81297 (10 μM) decreased dADP ($n = 28$, $^{**}P < 0.002$). Bath-applied forskolin (10 μM) reduced DHPG-induced dADP ($n = 8$, $^{**}P < 0.01$), and forskolin (10 μM) applied to internal electrode solution reduced synaptically triggered dADP ('Internal forskolin'; $n = 6$, $^{**}P < 0.01$). PKA inhibitor H89 (10 μM) and D1R antagonist SCH23390 (5 μM) blocked D1R-mediated inhibition. H89 alone (10 μM) had no effect ($n = 6$). Inset shows PKA inhibitor H89 blocking ability of SKF81297 to elevate PKA activity, using immunoblot for PKA phosphorylation site Thr34 on DARPP-32 ($n = 4$, $P < 0.05$). Slices were incubated for 10 min in DHPG (50 μM; control) and SKF81297 (10 μM) or for 1 h in H89 (10 μM) before incubation in DHPG and SKF81297. Bottom, superimposed representative traces showing modulation of DHPG-induced dADP by D1R agonist SKF81297 (10 μM; gray trace) compared to DHPG alone (black trace). Scale bars indicate 2 mV and 2 s. Inset shows five action potentials triggered by 50-Hz train of brief current stimulation before and after DHPG or DHPG + SKF81297. (**b**) DA (10 μM) inhibits synaptically evoked (30 × 50 Hz) dADP ('Norm dADP'; $n = 5$, $^{**}P < 0.01$) more than the fast EPSP ('EPSP'; $n = 5$, $^{*}P < 0.05$) integral either before or after compensation for the reduced fast EPSP. 'Norm EPSP' indicates restored fast EPSP in response to DA obtained by increasing stimulation intensity. (**c**) Representative traces show control EPSP, EPSP after DA ('DA') or after compensation of fast EPSP response by increasing stimulus intensity back to control level after DA ('Norm DA'). Scale bars show 2 mV and 5 ms. (**d**) Representative traces show synaptically triggered dADP control ('Control dADP'), after DA ('DA') and after increasing stimulus strength to restore fast EPSP to control levels ('Norm DA'). Scale bars show 2 mV and 2 s. Error bars represent s.e.m.

postsynaptic excitability using a physiologically relevant stimulus without presynaptic interference[32,35]. In saline-treated rats, D1R inhibition of the dADP using SKF81297 reduced the near-threshold conversion of simulated EPSPs to spikes, thus reducing the spike probability and narrowing the window in which the dADP was capable of boosting subthreshold inputs (**Fig. 7a**). The analysis of variance (ANOVA) statistics for this experiment were as follows: effect of SKF81297 in saline controls, $F_{1,40} = 25.99$ and $P < 0.0001$; effect of time (1–4 s), $F_{3,40} = 34.77$ and $P < 0.0001$; SKF81297 effect by time interaction, $F_{3,40} = 0.82$ and $P < 0.42$. Bonferroni post-test comparisons indicated significant differences between baseline and SKF81297 at 2 and 3 s ($P < 0.01$). Under normal conditions such D1R modulation may be important for filtering out stimuli that are not paired closely in time with the stimuli eliciting the initial burst, or for the reward-related termination of persistent activity.

In cocaine-treated rats given a short withdrawal, the ability of the dADP to convert near-threshold input to action potential output (spike probability) was significantly reduced for inputs occurring within 4 s after the initial burst (**Fig. 7b**). The ANOVA statistics for this experiment were as follows: group effect of saline versus cocaine baseline, $F_{1,68} = 30.04$ and $P < 0.0001$; effect of SKF81297, $F_{1,68} = 0.01$ and $P = 0.92$; effect of time (1–4 s), $F_{3,68} = 44.55$ and $P < 0.0001$; SKF81297 effect by time interaction, $F_{3,68} = 0.94$ and $P = 0.43$. Bonferroni post-test comparisons indicated a significant difference between saline and cocaine at 1 and 2 s after the burst ($P < 0.001$). No significant differences were detected between baseline and

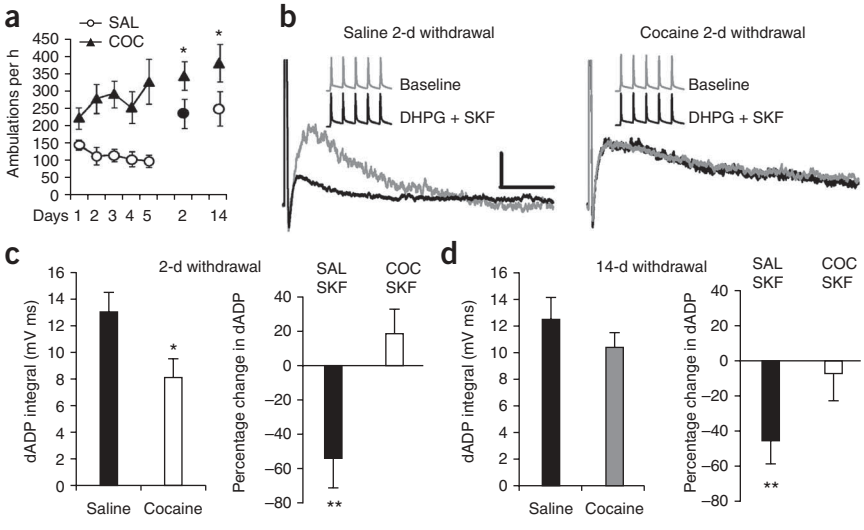

Figure 6 Repeated cocaine exposure reduces mGluR5- and burst-induced dADP and D1R modulation. (**a**) Behavioral sensitization measured by locomotor ambulation in rats treated with cocaine (COC; 15 mg kg^{-1} for 5 d) or saline (SAL; 0.9%, 1 ml kg^{-1}). Cocaine challenge (15 mg kg^{-1}) injections administered in both groups on withdrawal days 2 and 14 indicated behavioral sensitization in cocaine-treated group (saline versus cocaine; $n = 6$ per group, $^{*}P < 0.05$). (**b**) Superimposed representative traces show DHPG-mediated dADP triggered by brief bursts of five action potentials (50 Hz) at the early withdrawal (2-d) time point in rats treated with saline (left) or cocaine (right). SKF81297 ('DHPG + SKF'; 10 μM) reduced dADP in saline-treated but not cocaine-treated rats at the 2-d withdrawal point. Insets show burst stimulus used to evoke dADP in presence of DHPG (50 μM). (**c**) Left, average dADP integral response after 2 d of withdrawal in rats treated with saline ($n = 21$) or cocaine ($n = 22$), showing reduced dADP ($^{*}P < 0.03$). Right, average change in dADP integral in response to SKF81297 (10 μM) after 2 d of withdrawal from repeated treatment with saline ($n = 7$) or cocaine ($n = 8$, $^{**}P < 0.001$). (**d**) Left, no significant differences were observed in average dADP integral after 14 d of withdrawal in rats treated with saline ($n = 13$) or cocaine ($n = 15$; $P > 0.05$). Right, D1R-mediated inhibition (SKF81297, 10 μM) of dADP remained significantly reduced in cocaine-treated ('COC SKF'; $n = 11$, $^{**}P < 0.03$) compared to saline-treated ('SAL SKF'; $n = 11$) rats at 14-d withdrawal point. Error bars represent s.e.m.

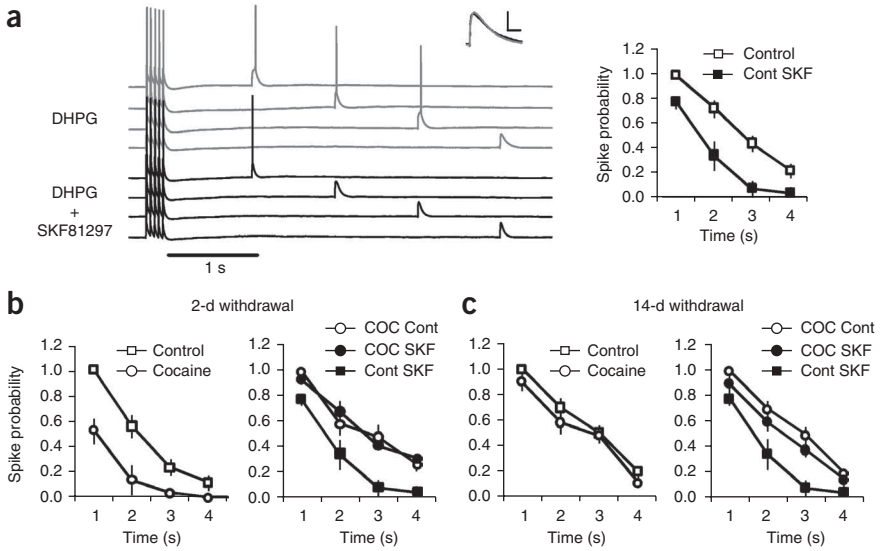

Figure 7 Repeated cocaine treatment reduces the mGluR5- and burst-mediated conversion of subthreshold input to suprathreshold action potential output and D1R modulation. (**a**) Left, whole-cell patch-clamp recording of layer 5 pyramidal neuron given burst of five suprathreshold simulated synaptic current injections at 20 Hz, followed by single subthreshold simulated current injection delivered at 85% of threshold at times from 1 s to 4 s after burst in presence of DHPG (50 μM; gray traces) and after SKF81297 (10 μM; black traces). DHPG elicited a dADP that converted fast subthreshold input to suprathreshold spike output in the first 3 s after burst. Inset shows superimposed fast EPSP responses before and after DHPG (gray trace) and SKF81297 (black trace) when measured before burst of five action potentials. Scale bar shows 5 mV and 10 ms. Right, average spike probability in response to subthreshold simulated postsynaptic input in presence of DHPG (50 μM; 'Control') and SKF81297 (10 μM; 'Cont SKF'; $n = 8$, $P < 0.01$ at 2 and 3 s). (**b**) Left, short (2-d) withdrawal from repeated cocaine treatment reduced spike probability (saline control, $n = 8$; cocaine, $n = 11$; $P < 0.001$ at 1 and 2 s). Right, normalized spike probability after DHPG and SKF81297 in saline-treated control group ('Cont SKF'; $n = 8$) and cocaine-treated group given DHPG alone ('COC Cont') or DHPG and SKF81297 ('COC SKF'). (**c**) Left, late (14-d) withdrawal from repeated cocaine treatment did not alter burst-triggered dADP (saline control, $n = 6$; cocaine, $n = 6$; $P > 0.05$). Right, lack of D1R modulation of normalized spike probability for cocaine-treated group in response to DHPG ('COC Cont') and after SKF81297 ('COC SKF'; $P > 0.05$) compared to saline or untreated controls ('Cont SKF'). The 'Cont SKF' group from panel **a** is shown in panels **b** and **c** for comparison. Error bars represent s.e.m.

SKF81297 in the cocaine group at any time point ($P > 0.05$). This cocaine-induced reduction in spike probability recovered after a long-term withdrawal period, but the loss of D1R function remained substantially reduced compared to saline controls (**Fig. 7c**). The ANOVA statistics were as follows: group effect of saline versus cocaine baseline, $F_{1,40} = 0.79$ and $P = 0.38$; effect of time (1–4 s), $F_{3,40} = 13.60$ and $P < 0.0001$; group by time interaction, $F_{3,40} = 0.06$ and $P = 0.98$; effect of SKF81297, $F_{1,40} = 3.13$ and $P = 0.084$; effect of time (1–4 s) effect, $F_{3,40} = 50.81$ and $P < 0.0001$; drug by time interaction effect, $F_{3,40} = 0.19$ and $P = 0.90$. Bonferroni post-test comparisons indicated no significant differences between saline and cocaine groups or in the baseline and SKF81297 comparison in the cocaine group at any time point ($P > 0.05$).

The cocaine-induced increase in input resistance and spike output (**Supplementary Table 1**) in response to prolonged current injections indicated increased excitability, whereas the reduced burst-triggered dADP suggested a reduced *in vivo* ability to maintain a stable persistent dADP state in the absence of sustained excitatory drive. These cocaine-induced changes may bias the PFC neurons to favor only strong sustained input lasting seconds while weakening their ability to shift to a persistent output mode in response to brief burst activation.

DISCUSSION

Here we described a short-lived and rapidly reversible cellular mechanism of persistent activity that was initiated by strong synaptic activation of mGluR5 and bursts of action potentials. Classic cellular models of synaptic memory storage, such as long-term potentiation and long-term depression, are unable to account for transient memory because the cellular cascades that produce long-term potentiation and long-term depression turn on and off too slowly to function as a temporary (for example, seconds) memory storage buffer. In contrast, persistent activity might provide a mechanism for a temporary working memory buffer, as it is capable of converting brief, strong, 'information bearing' input into enduring action potential output that decays over several seconds and then resets when the response has been made and the stored information is no longer needed.

Recurrent network computational models are capable of modeling short-term persistent activity but thus far have lacked a plausible biophysical mechanism[6,7]. The robustness and tuning of conductance-based models can be improved by artificially lengthening the synaptic decay time constant beyond ~100 ms. The long-lasting mGluR5-mediated depolarization, with a time constant of ~3 s, provides a potential mechanism that enables synaptically triggered action potential output to be maintained for several seconds despite diminishing excitatory input, even in the presence of brief hyperpolarization.

The group 1 mGluR1 and mGluR5 agonists (ACPD or DHPG) induce an action potential–triggered nonselective cation current that produces a dADP in the somatosensory cortex[14], subiculum[9], entorhinal cortex[36] and cerebellum[15], although the ion channel mechanism remains unknown. In the cerebellum, stimulation of mGluR1 cascades leads to activation of the nonselective transient cation channel TRPC3, causing slow inward currents in Purkinje neurons[15]. The mammalian TRPC family contains seven members (TRPC1–7) that are activated by PLC[37]. We have shown that TRPC4 and TRPC5 are the predominant variants in the PFC, and their mRNA and protein expression correlates with the group 1 mGluR–mediated, burst-elicited dADP[9]. Group 1 mGluRs include mGluR1 and mGluR5. It is mGluR5, rather than mGluR1, that is predominantly expressed on deep-layer pyramidal neurons within the PFC[38]. mGluR5 is located in the perisynaptic region of the postsynaptic membrane and is activated by bursts of action potentials[11,39]. We propose that mGluR5 activation of layer 5 pyramidal neurons in the PFC leads to action potential–dependent, TRPC-like depolarization underlying persistent activity[8,9,40].

As a signaling mode, bursting output is notable because it may enhance detection of new and salient stimuli in goal-directed behaviors and facilitate the induction of synaptic plasticity[41]. In fact, it has been shown that mGluR5 works with NMDA receptors in deep-layer pyramidal neurons to modulate bursting action potential output[10,11].

mGluR5 blockade decreases the spontaneous burst activity of the majority of PFC neurons, but does not alter the nonbursting spontaneous activity of PFC neurons, indicating a preferential role for mGluR5 in regulating bursting spike output.

The burst-triggered, mGluR5-induced dADP underlying persistent activity was reduced by D1R-mediated PKA activation. DA is an important modulator of PFC attention and working memory function. In the PFC, other forms of synaptic memory (long-term potentiation and long-term depression) have been reported to be crucially dependent on DA receptor signaling[13]. DA normally exerts its cellular effects by activation of D1R and/or D2R. Pyramidal neurons in the PFC express both types of receptors, although D1R is expressed in 20-fold higher amounts than is D2R[42]. In the rat, layer 5 receives the strongest DA input, as shown by electron microscopy of DA terminals[17]. Consistent with an important role for D1R activation in the PFC, we found that D1R stimulation decreased the burst-triggered depolarization. The implications of the DA-induced reduction of the dADP underlying persistent activity are unclear, but it is possible that D1R activation associated with reward presentation is involved in the termination of a persistently activated state, or it may increase the signal-to-noise ratio by selecting only the strongest synaptic inputs for persistent activation.

A growing body of research indicates diminished PFC function after chronic psychostimulant use in humans and animal models[3,4,24,25,27,35,43–45]. For example, cocaine abusers manifest behavioral abnormalities similar to those observed in patients with orbitofrontal damage, such as choosing immediate high-risk rewards, despite knowledge of the future negative consequences of the decision[44]. Human brain imaging studies of cocaine-dependent individuals show increased functional magnetic resonance imaging activity of the PFC after cocaine alone and in response to cocaine-paired cues[45,46]. In the rodent PFC, glutamatergic transmission is crucial for cocaine-primed reinstatement of drug-seeking behavior and is mediated by a glutamatergic projection from the PFC to the nucleus accumbens[47]. Furthermore, mGluR5-mediated transmission is necessary for normal psychostimulant response to cocaine (**Supplementary Fig. 5** online)[12]. Cocaine self-administration produces deficits in impulsivity and attention that is correlated with changes in mGluR5 mRNA in the frontal cortex[3]. In addition, repeated exposure to D-amphetamine produces a progressive enhancement of PFC inhibition of neurons that respond to task-related events and is correlated with decline in working memory performance[27]. As previously reported[24,25], we found that withdrawal from repeated exposure to psychostimulant drugs produced changes in the intrinsic excitability of layer 5 pyramidal neurons (**Supplementary Table 1**). Moreover, the mGluR5-mediated dADP mechanism was impaired during the abstinence period after repeated cocaine exposure, which would be predicted to diminish intrinsic, persistent PFC activity.

Overall, our findings implicate the mGluR5 dADP as an intrinsic cellular mechanism capable of initiating persistent activity. As in working memory tasks, the dADP is reduced by mGluR5 antagonists, modulated by D1R and PKA activation and diminished after repeated cocaine exposure and withdrawal. In addition to drug addiction, disruptions of PFC persistent activity resulting from impaired mGluR5–DA receptor interactions may have an important role in pathologies of frontal cortical attention and working memory, including attention deficit disorder, schizophrenia and post-traumatic stress disorder[44,48,49].

METHODS

Animals. Male rats and mice (Charles River) were housed in groups in a temperature- and humidity-controlled vivarium under a 12-h light-dark cycle. Food and water were available *ad libitum*. The mGluR1- and mGluR5-knockout mice were obtained from K. Huber and were 5–6 weeks old. Rats arrived at 4 weeks of age and were allowed to acclimate for 3–5 d before being used for experiments. All animal procedures were done in accordance with the National Institutes of Health Guide for the Care and Use of Laboratory Animals and were approved by the Institutional Animal Care and Use Committee.

Slice preparation. Animals were perfused under halothane anesthesia with cold, oxygenated ACSF containing 124 mM NaCl, 2.5 mM KCl, 26 mM $NaHCO_3$, 2 mM $MgCl_2$, 2 mM $CaCl_2$ and 10 mM glucose (pH 7.4; 310 mOsm l^{-1}). After decapitation, the brain was removed and immersed in ice-cold ACSF. The portion containing the PFC was glued onto the specimen holder and submerged in the buffer tray of a VT1000S vibratome (Leica Microsystems) containing cold, oxygenated ACSF. Brain slices were cut in 300-μm-thick sections and transferred to a custom-made nylon support chamber filled with oxygenated ACSF. Slices where kept in the chamber at 34 °C for 30 min and then transferred to room temperature (23 °C) until used for recording 1–4 h later.

Electrophysiological recordings. Brain slices were placed in a custom temperature-controlled (32–35 °C) recording chamber and placed under an Olympus BX-51WI upright light microscope on a Vibraplane 9100/9200 Series vibration isolation table (Kinetic Systems Inc., MA). The slice was perfused by gravity-fed, oxygenated ACSF at a flow rate of 2–3 ml min^{-1}. Whole-cell patch-clamp recordings were obtained from layer 5 PFC pyramidal neurons and visually identified on a Sony monitor using differential interference contrast optics and a Dage-MTI (Dage-MTI, Michigan City, IN) camera. After the formation of a tight seal (>1 GΩ), a small whole-cell configuration was obtained. A patch-clamp amplifier (BVC 700A, current clamp; 3900A, voltage clamp; Dagan Corporation, MN) was used for current- and voltage-clamp recording. Voltage signals were digitized with an InstruTech ITC-18 analog-to-digital converter. The data were stored in a Pentium computer using IGOR Pro software (WaveMetrics Inc., OR). Recordings were accepted for study if the neuron's resting membrane potential was more negative than –60 mV, had overshooting spikes and a series resistance less than 30 MΩ. Slices were perfused with ACSF containing 2.5 mM kynurenic acid (Sigma-Aldrich, MO), 2 μM SR 95531(Tocris Bioscience, MO) and 1 μM atropine to block ionotropic (NMDA and AMPA) and $GABA_A$ receptors. At the end of each experiment, the slice was placed in 4% paraformaldehyde solution and kept at 4 °C until histological processing.

Current-clamp recording. All current and voltage-clamp recordings were obtained with glass electrodes (2–3 MΩ) in a whole-cell configuration. Recording pipettes (2–4 MΩ) were pulled from Corning 7056 borosilicate glass capillaries with a horizontal pipette puller (Flaming/Brown P-97, Sutter Instruments) and filled with 115 mM potassium gluconate, 10 mM HEPES, 20 mM KCl, 2 mM $MgCl_2$, 3 mM Na_2ATP, 0.3 mM Na_2GTP and 0.1% biocytin (pH 7.3, 280 mOsm). Cells in current clamp (I_{Clamp}) were recorded with a holding potential of –65 mV unless otherwise noted. Synaptic responses were recorded in response to stimulation of the layer 3 axons using a 50-Hz bipolar stimulus (5 or 30 pulses). To monitor the input resistance, a series of 600-ms step pulses from –200 pA to +300 pA were delivered, and the steady-state voltage deflection was calculated. To trigger the dADP, a train of five suprathreshold 5-ms step pulses delivered at 50 Hz was used. The current injection trains were applied every 30 s. Unless otherwise noted, all experiments were done using the above train protocol. When traces were obtained for dADP measurements, the membrane potential of the cell was held at –67 mV. All recordings were made in the presence of kynurenic acid (2 mM) to block ionotropic glutamate (~90% block) and SR 95531 (2 μM) to block $GABA_A$ receptors and atropine to block muscarinic acetylcholine receptors.

The simulated synaptic current injections (EPSCs) were injected into the soma through the recording patch pipette, followed 400 ms later by a 5-ms square step pulse scaled to half the simulated EPSC amplitude to verify accurate bridge balance and capacitance compensation. We set the simulated EPSCs kinetics with a rise time of 0.2 ms and a decay time of 6 ms, yielding simulated EPSPs that closely resembled actual EPSPs[32,35].

Voltage-clamp recordings. A cesium gluconate–based internal was used to record I_{DHPG} (115 mM cesium gluconate, 10 mM sodium phosphocreatine, 10 mM HEPES, 2 mM EGTA, 2 mM MgATP, 0.3 mM Na_2GTP and 20 mM CsCl). Membrane potentials reported were not corrected for a 8 mV liquid junction potential present when using gluconate-based internal solutions. The recorded current was filtered at 3 kHz and sampled at 50 kHz. Data analysis was done with IGOR pro software. Currents were acquired using leak subtraction and capacitance and series resistance compensation. Analysis was done using averages of two to ten responses. Values are reported as mean ± s.e.m. DHPG (100 μM) was puffed on for 1 s, and the corresponding inward current (I_{DHPG}) was measured at a holding potential of –65 mV.

Calcium imaging. Intracellular Ca^{2+} Measurement–HEK293 cells stably expressing mGluR5 were seeded in wells of a 96-well plate for 20–24 h to achieve about 95% confluence. After washing with normal extracellular solution containing (in mM): NaCl 140, KCl 5, CaCl2 2, MgCl2 1, glucose 10, HEPES 15, pH 7.4, cells were loaded with 5 μM Fluo-4 AM in normal extracellular solution supplemented with 2 mM probenecid and 0.1% pluronic F-127 at 37 °C in darkness for about 45 min. In order to suppress the constitutive activity of the receptor, 2-methyl-6 [phenylethynyl]-pyridine (MPEP, 1 ìM) was included in the cell culture medium. An automated florescence plate reader integrated with a robotic 8-channel fluid handling system, Flex Station (Molecular Devices, Sunnyvale, CA), was used to monitor the intracellular [Ca^{2+}] as described before[50].

Drugs. ACPD, DHPG, LY341495, LY367385, MPEP and SR95531 were obtained from Tocris Bioscience. DHPG, kynurenic acid, DA, SKF81297, forskolin, quinpirole and atropine were obtained from Sigma. Drugs were dissolved in H_2O or ACSF.

Analysis. The amplitude of the dADP was calculated by measuring the difference between the average membrane potential 50 ms before the stimulus onset and the membrane potential peak after the spike train. The decay phase of the dADP was fitted by a single exponential function ($y = a \times e^{-bx}$), and the time constant of decay was $1/b$. Throughout the experiment, the input resistance of the cell was monitored using a 600-ms step pulse protocol with current injections from –100 pA to +100 pA. The points of the potential difference between the V_m and the response potential were plotted against the current used for the points between –100 pA and +100 pA. The points were fitted to a line ($y = ax + b$), and input resistance was the slope of that line.

Histology. After recording, the slice was removed from the recording chamber, placed in 4% paraformaldehyde, washed with PBS, incubated in a solution containing 10% methanol and 3% hydrogen peroxide dissolved in PBS for 30 min, washed again and incubated in avidin-biotin complex reagent solution for at least 2 h at 23 °C. After another wash, the slice was incubated in 0.1% gluteraldehyde for 4 min, washed and incubated in diaminobenzidine solution and mounted with Mowiol and a cover slip. Slices were observed under an Olympus BX-51WI microscope to determine the cellular morphology. After recording, each cell was processed for morphological verification of pyramidal neuronal morphology and placement in layer 5 (**Fig. 1a**).

Locomotor activity. Mice were habituated to the locomotor apparatus for 1 h before testing on each day. Mice were tested for control locomotor activity for 2 d of saline injections before an ascending dosing regimen of cocaine challenge injections (10, 20 and 40 mg kg^{-1}; 2 ml kg^{-1} volume). Between cocaine injection days, mice were tested with saline to avoid conditioning to the effects of cocaine.

Rats were allowed to acclimate for at least 5 d and then assigned randomly into two groups that received an intraperitoneal injection of either saline (1 ml kg^{-1}) or cocaine HCl (15 mg kg^{-1}) for 5 d. After a 2- or 14-d withdrawal period, rats were tested with a challenge injection (15 mg kg^{-1}) to probe for locomotor sensitization. For the five treatment days and challenge days, locomotor activity was recorded during the light cycle in a darkened circular test chamber with a 12-cm-wide runway, equipped with four pairs of photocells located at 90° intervals around the 1.95-m perimeter.

Statistics. ANOVA followed by paired or unpaired t tests were used as appropriate. A result was considered significant when $P < 0.05$ using a two-tailed analysis. Bonferroni correction was used to hold P constant at 0.05 for multiple comparisons among treatment means.

Note: Supplementary information is available on the Nature Neuroscience website.

ACKNOWLEDGMENTS

We thank K. Huber (University of Texas Southwestern Medical Center at Dallas) for the mGluR1 and mGluR5 wild-type and knockout mice. This work was supported by National Institute on Drug Abuse grant R01-DA24040 (to D.C.C.), NIDA K award K-01DA017750 (to D.C.C.), a NARSAD Young Investigator award (to D.C.C.), National Institute on Drug Abuse institutional training grant T32-DA7290 (to M.A.F.), the Onassis Public Benefit Foundation (to K.S.), a Gulf War Syndrome contract from the US Department of Veterans Affairs and Veterans Affairs IDIQ contract VA549-P-0027 (awarded and administered by the Dallas, Texas, VA Medical Center). This paper is dedicated to the memory of Francis J. White, a close friend and mentor.

AUTHOR CONTRIBUTIONS

K.S., F.-M.L., E.D.O. and D.C.C. conducted the patch-clamp experiments. K.S. and D.C.C. wrote the manuscript. M.A.F. performed behavioral experiments. C.P. carried out immunoblot experiments, and R.X. and M.X.Z. performed calcium imaging experiments in HEK cells. F.J.W. and D.C.C. supervised the project.

Published online at http://www.nature.com/natureneuroscience/
Reprints and permissions information is available online at http://www.nature.com/reprintsandpermissions/

1. Goldman-Rakic, P.S. Regional and cellular fractionation of working memory. *Proc. Natl. Acad. Sci. USA* **93**, 13473–13480 (1996).
2. Funahashi, S. & Takeda, K. Information processes in the primate prefrontal cortex in relation to working memory processes. *Rev. Neurosci.* **13**, 313–345 (2002).
3. Winstanley, C.A. *et al.* DeltaFosB induction in orbitofrontal cortex mediates tolerance to cocaine-induced cognitive dysfunction. *J. Neurosci.* **27**, 10497–10507 (2007).
4. George, O., Mandyam, C.D., Wee, S. & Koob, G.F. Extended access to cocaine self-administration produces long-lasting prefrontal cortex-dependent working memory impairments. *Neuropsychopharmacology* **33**, 2474–2482 (2008).
5. Goldman-Rakic, P.S. Cellular basis of working memory. *Neuron* **14**, 477–485 (1995).
6. Seung, H.S. *et al.* Stability of the memory of eye position in a recurrent network of conductance-based model neurons. *Neuron* **26**, 259–271 (2000).
7. Wang, X.J. Synaptic reverberation underlying mnemonic persistent activity. *Trends Neurosci.* **24**, 455–463 (2001).
8. Egorov, A.V., Hamam, B.N., Fransén, E., Hasselmo, M.E. & Alonso, A.A. Graded persistent activity in entorhinal cortex neurons. *Nature* **420**, 173–178 (2002).
9. Fowler, M.A., Sidiropoulou, K., Ozkan, E.D., Phillips, C.W. & Cooper, D.C. Corticolimbic expression of TRPC4 and TRPC5 channels in the rodent brain. *PloS ONE* **2**, e573 (2007).
10. Homayoun, H., Stefani, M.R., Adams, B.W., Tamagan, G.D. & Moghaddam, B. Functional interaction between NMDA and mGlu5 receptors: effects on working memory, instrumental learning, motor behaviors, and dopamine release. *Neuropsychopharmacology* **29**, 1259–1269 (2004).
11. Homayoun, H. & Moghaddam, B. Bursting of prefrontal cortex neurons in awake rats is regulated by metabotropic glutamate 5 (mGlu5) receptors: rate-dependent influence and interaction with NMDA receptors. *Cereb. Cortex* **16**, 93–105 (2006).
12. Chiamulera, C. *et al.* Reinforcing and locomotor stimulant effects of cocaine are absent in mGluR5 null mutant mice. *Nat. Neurosci.* **4**, 873–874 (2001).
13. Otani, S. *et al.* Dopamine receptors and groups I and II mGluRs cooperate for long-term depression induction in rat prefrontal cortex through converging postsynaptic activation of MAP kinases. *J. Neurosci.* **19**, 9788–9802 (1999).
14. Greene, C.C., Schwindt, P.C. & Crill, W.E. Properties and ionic mechanisms of a metabotropic glutamate receptor-mediated slow afterdepolarization in neocortical neurons. *J. Neurophysiol.* **72**, 693–704 (1994).
15. Hartmann, J. *et al.* TRPC3 channels are required for synaptic transmission and motor coordination. *Neuron* **59**, 392–398 (2008).
16. Groenewegen, H.J. Organization of the afferent connections of the mediodorsal thalamic nucleus in the rat, related to the mediodorsal-prefrontal topography. *Neuroscience* **24**, 379–431 (1988).
17. Carr, D.B. & Sesack, S.R. Dopamine terminals synapse on callosal projection neurons in the rat prefrontal cortex. *J. Comp. Neurol.* **425**, 275–283 (2000).
18. Watanabe, M., Kodama, T. & Hikosaka, K. Increase of extracellular dopamine in primate prefrontal cortex during a working memory task. *J. Neurophysiol.* **78**, 2795–2798 (1997).
19. Phillips, A.G., Ahn, S. & Floresco, S.B. Magnitude of dopamine release in medial prefrontal cortex predicts accuracy of memory on a delayed response task. *J. Neurosci.* **24**, 547–553 (2004).

20. Vijayraghavan, S., Wang, M., Birnbaum, S.G., Williams, G.V. & Arnsten, A.F. Inverted-U dopamine D1 receptor actions on prefrontal neurons engaged in working memory. *Nat. Neurosci.* **10**, 376–384 (2007).
21. Williams, G.V. & Goldman-Rakic, P.S. Modulation of memory fields by dopamine D1 receptors in prefrontal cortex. *Nature* **376**, 572–575 (1995).
22. Wang, J. & O'Donnell, P. D(1) dopamine receptors potentiate NMDA-mediated excitability increase in layer 5 prefrontal cortical pyramidal neurons. *Cereb. Cortex* **11**, 452–462 (2001).
23. Yang, C.R. & Seamans, J.K. Dopamine D1 receptor actions in layers 5–6 rat prefrontal cortex neurons in vitro: modulation of dendritic-somatic signal integration. *J. Neurosci.* **16**, 1922–1935 (1996).
24. Dong, Y. *et al.* Cocaine-induced plasticity of intrinsic membrane properties in prefrontal cortex pyramidal neurons: adaptations in potassium currents. *J. Neurosci.* **25**, 936–940 (2005).
25. Peterson, J.D., Wolf, M.E. & White, F.J. Repeated amphetamine administration decreases D1 dopamine receptor-mediated inhibition of voltage-gated sodium currents in the prefrontal cortex. *J. Neurosci.* **26**, 3164–3168 (2006).
26. Young, C.E. & Yang, C.R. Dopamine D1/D5 receptor modulates state-dependent switching of soma-dendritic Ca^{2+} potentials via differential protein kinase A and C activation in rat prefrontal cortical neurons. *J. Neurosci.* **24**, 8–23 (2004).
27. Homayoun, H. & Moghaddam, B. Progression of cellular adaptations in medial prefrontal and orbitofrontal cortex in response to repeated amphetamine. *J. Neurosci.* **26**, 8025–8039 (2006).
28. Hanes, D.P. & Schall, J.D. Neural control of voluntary movement initiation. *Science* **274**, 427–430 (1996).
29. Rainer, G., Asaad, W.F. & Miller, E.K. Memory fields of neurons in the primate prefrontal cortex. *Proc. Natl. Acad. Sci. USA* **95**, 15008–15013 (1998).
30. Rae, M.G. *et al.* Role of Ca2+ stores in metabotropic l-glutamate receptor-mediated supralinear Ca^{2+} signaling in rat hippocampal neurons. *J. Neurosci.* **20**, 8628–8636 (2000).
31. Nakamura, T. *et al.* Synergistic release of Ca^{2+} from IP3-sensitive stores evoked by synaptic activation of mGluRs paired with backpropagating action potentials. *Neuron* **24**, 727–737 (1999).
32. Cooper, D.C., Chung, S. & Spruston, N. Output-mode transitions are controlled by prolonged inactivation of sodium channels in pyramidal neurons of subiculum. *PLoS Biol.* **3**, e175 (2005).
33. Gao, W.J., Krimer, L.S. & Goldman-Rakic, P.S. Presynaptic regulation of recurrent excitation by D1 receptors in prefrontal circuits. *Proc. Natl. Acad. Sci. USA* **98**, 295–300 (2001).
34. Madeja, M. Do neurons have a reserve of sodium channels for the generation of action potentials? A study on acutely isolated CA1 neurons from the guinea-pig hippocampus. *Eur. J. Neurosci.* **12**, 1–7 (2000).
35. Cooper, D.C. *et al.* Psychostimulant-induced plasticity of intrinsic neuronal excitability in ventral subiculum. *J. Neurosci.* **23**, 9937–9946 (2003).
36. Yoshida, M., Fransén, E. & Hasselmo, M.E. mGluR-dependent persistent firing in entorhinal cortex layer III neurons. *Eur. J. Neurosci.* **28**, 1116–1126 (2008).
37. Montell, C. The TRP superfamily of cation channels. *Sci. STKE* **2005**, re3 (2005).
38. Lopez-Bendito, G., Shigemoto, R., Fairen, A. & Lujan, R. Differential distribution of group I metabotropic glutamate receptors during rat cortical development. *Cereb. Cortex* **12**, 625–638 (2002).
39. Lujan, R. *et al.* Perisynaptic location of metabotropic glutamate receptors mGluR1 and mGluR5 on dendrites and dendritic spines in the rat hippocampus. *Eur. J. Neurosci.* **8**, 1488–1500 (1996).
40. Hagenston, A.M., Fitzpatrick, J.S. & Yeckel, M.F. mGluR-mediated calcium waves that invade the soma regulate firing in layer V medial prefrontal cortical pyramidal neurons. *Cereb. Cortex* **18**, 407–423 (2008).
41. Cooper, D.C. The significance of action potential bursting in the brain reward circuit. *Neurochem. Int.* **41**, 333–340 (2002).
42. Gaspar, P., Bloch, B. & Le Moine, C. D1 and D2 receptor gene expression in the rat frontal cortex: cellular localization in different classes of efferent neurons. *Eur. J. Neurosci.* **7**, 1050–1063 (1995).
43. Zhang, X.F., Hu, X.T. & White, F.J. Whole-cell plasticity in cocaine withdrawal: Reduced sodium currents in nucleus accumbens neurons. *J. Neurosci.* **18**, 488–498 (1998).
44. Bechara, A. *et al.* Decision-making deficits, linked to a dysfunctional ventromedial prefrontal cortex, revealed in alcohol and stimulant abusers. *Neuropsychologia* **39**, 376–389 (2001).
45. Grant, S. *et al.* Activation of memory circuits during cue-elicited cocaine craving. *Proc. Natl. Acad. Sci. USA* **93**, 12040–12045 (1996).
46. Breiter, H.C. *et al.* Acute effects of cocaine on human brain activity and emotion. *Neuron* **19**, 591–611 (1997).
47. McFarland, K., Lapish, C.C. & Kalivas, P.W. Prefrontal glutamate release into the core of the nucleus accumbens mediates cocaine-induced reinstatement of drug-seeking behavior. *J. Neurosci.* **23**, 3531–3537 (2003).
48. Perlstein, W.M. *et al.* Relation of prefrontal cortex dysfunction to working memory and symptoms in schizophrenia. *Am. J. Psychiatry.* **158**, 1105–1113 (2001).
49. Koenigs, M. *et al.* Focal brain damage protects against post-traumatic stress disorder in combat veterans. *Nat. Neurosci.* **11**, 232–237 (2008).
50. Hu, H.Z. *et al.* 2-aminoethoxydiphenyl borate is a common activator of TRPV1, TRPV2, and TRPV3. *J. Biol. Chem.* **279**, 35741–35748 (2004).